

Electrical transport properties of V_3Si , V_5Si_3 , and VSi_2 thin films

F. Nava,* O. Bisi,* and K. N. Tu

IBM Thomas J. Watson Research Center, Yorktown Heights, New York 10598

(Received 24 February 1986)

Resistivity measurements in a wide temperature range (2–1100 K) have been performed on thin films of V_3Si , V_5Si_3 , and VSi_2 formed on an inert substrate. An anomalous resistivity behavior has been observed in these metallic compounds: The resistivity deviates from linearity and approaches a saturation value at the higher temperatures. The resistivity data can be fitted quite well to a phenomenological expression based on the idea that a limiting resistivity is reached when the electron mean free path is of the order of the interatomic spacing. The electron mean free paths, which have been computed from the experimental data, lend support to the above idea. The saturation phenomenon in V_3Si and V_5Si_3 compounds is characterized by a limiting resistivity of the same magnitude as observed in several *A15* materials and in the Mooij correlation, yet in VSi_2 the resistivity saturates to a much higher value. The V_3Si is a superconductor with a transition temperature around 15 K and a residual resistivity ratio of 10.6. On the other hand, V_5Si_3 and VSi_2 thin compound films do not show superconductivity state down to 2 K. The temperature dependence of the Hall coefficient gives evidence of a complex and different electronic structure of the three compounds.

I. INTRODUCTION

Current interest in the structure and electrical properties of silicides and their interfaces is not only due to their applications in microelectronics devices as contacts and field-effect transistor gates¹ but also due to the possibility of controlling their structure and composition for a systematic scientific study.^{2–5} Attempts have been made to understand the temperature (T) dependence of the resistivity (ρ) of silicides on a fundamental level and to determine the transport parameters. Several refractory metal-silicide thin films, characterized by having a high resistivity value at room temperature, show an anomalous metallic behavior at high temperatures; the ρ versus T curve flattens out with a negative deviation from linearity and approaches a saturation value as temperature increases.^{2,5} The resistivity saturation phenomenon has been observed in many high- T_c superconductors which have a cubic⁶ and *A15* crystal structure,^{7,8} and has been associated with the breakdown of the classical Boltzmann theory when the mean free path is approaching interatomic distances.^{9–12} To describe this phenomena a shunt-resistor model has been proposed and it has been found to fit the data quite well.^{9,13–16} To analyze the same phenomenon in the electrical transport of silicides, we measured the temperature dependence of the resistivity of V_3Si , V_5Si_3 , and VSi_2 thin films in a wide temperature range (2–1100 K) in order to reveal the nonlinear temperature dependence and the quasisaturation of ρ at higher temperatures.

These three compounds were chosen because they represent all the intermetallic compounds in the V-Si binary system and because they have different crystal structure. While V_3Si has the *A15* cubic structure, V_5Si_3 and VSi_2 have a tetragonal and a hexagonal structure, respectively. Furthermore, V_3Si is a well-studied high- T_c superconducting compound, its temperature-dependent resistivity electronic structure in the vicinity of the Fermi

level and phonon dispersion relations are available in the literature,^{17–21} so we have a reliable reference for comparison.

The effect of defects and impurities on the saturation behavior has also been studied by adding excess Si into the compound VSi_2 , and we found that it affects the saturation behavior by increasing both the residual resistivity and electron-phonon resistivity parameter.

II. EXPERIMENTAL

Amorphous thin films of vanadium-silicon alloys with three different compositions were prepared by simultaneous evaporation of vanadium and silicon in a dual electron-gun evaporation system. Typical rates were 4 Å/sec for vanadium and 12 Å/sec for silicon. The background pressure during evaporation was maintained at 2×10^{-7} Torr.

The composition of the alloy films was selected in order to form the V_3Si , V_5Si_3 , and VSi_2 compounds, respectively, by a subsequent annealing. Thicknesses of 1000, 880, and 1050 Å have been measured for V_3Si , V_5Si_3 , and VSi_2 , respectively, after their heat treatment at 900°C for 30 min. In the case of VSi_2 , the alloy film was deliberately enriched in silicon in order to increase the content of the defects and impurity inside the film. Stoichiometric VSi_2 films were formed by reacting bilayer vanadium-silicon films; amorphous silicon films 2500 Å thick and vanadium films 870 Å thick were evaporated consecutively at pressures below 4×10^{-7} Torr and annealed subsequently at 900°C for 30 min. The specific thicknesses of vanadium and silicon were selected in order to form a stoichiometric VSi_2 film of 2700 Å thick. We recall that VSi_2 is the first phase to form by reacting V and Si.

For electrical characterization the specimens were prepared in a van der Pauw configuration by deposition of

the thin films on oxidized silicon wafers through metallic masks. To study the temperature dependence of electrical resistivity from room temperature to higher temperature (1100 K), specimens which had been heat treated at 900°C for 30 min were utilized. Since heat treatment for a longer time (5 h) does not change the room-temperature value of the resistivity, we assume this is an indication that they have been fully crystallized after 30 min at 900°C. The same heat-treated specimens were also used to study the *in situ* electrical resistivity and Hall voltage temperature dependence from room temperature to low temperatures.

For room-temperature through high-temperature measurements, the specimens were heat treated at a rate of 1.5°C/min in a quartz tube furnace with a constant flow of purified helium gas. Temperature dependence of the *in situ* electric resistivity was made by four spring-loaded tantalum wires contacted to the pads of the van der Pauw pattern. The temperature was measured by a calibrated Chromel-Alumel thermocouple to within ± 1 K. The thermocouple was attached to the specimen holder and was in direct contact with the back side of the specimen.

For low-temperature measurement, the contacts were formed by indium soldering thin copper wires to the four contact pads of the van der Pauw pattern, and the measurements were performed in a liquid-helium cryostat. The specimens were mounted on a copper block located in a double vacuum chamber which enabled the specimen temperature to be varied from 2 to 300 K. The temperature was measured with a calibrated germanium-resistance thermometer to within ± 0.2 K in the temperature range 2–97 K, and with a calibrated iron-Constantan thermocouple to within ± 1 K in the temperature range 97–300 K.

The error in the absolute values of ρ was estimated to be $\sim 4\%$, due to the uncertainty (± 50 Å) in the film-thickness measurement. Variations in the resistivity of a single specimen could be determined with an uncertainty of 8%.

Hall voltage measurements below room temperature were performed with a variable-temperature cold-end system (Air-Product Model No. CS-202). The temperature was measured with a calibrated (Au-0.07 at. % Fe—Chromel thermocouple to within ± 0.5 K (Scientific Instrument Inc. Model No. C907F) in the temperature range 14–350 K. Both dc and ac techniques were used to measure the Hall voltage. The magnetic field was 8 kG and the Hall voltage was linear with the magnetic field up to this value. Low values of current were employed and the resistivity and Hall-coefficient measurements showed a linear dependence on the current in the range utilized.

Film-thickness and depth-composition analysis were performed using Rutherford backscattering spectrometry (RBS) with a 2.3-MeV $^4\text{He}^+$ ion beam. Crystalline phases and microstructures present in the films were identified by glancing incidence x-ray diffraction (XRD), transmission electron diffraction (TED), and transmission electron microscopy (TEM). These measurements were made directly on the van der Pauw structure, with the backside silicon and silicon oxide etched off for TEM and TED examination.

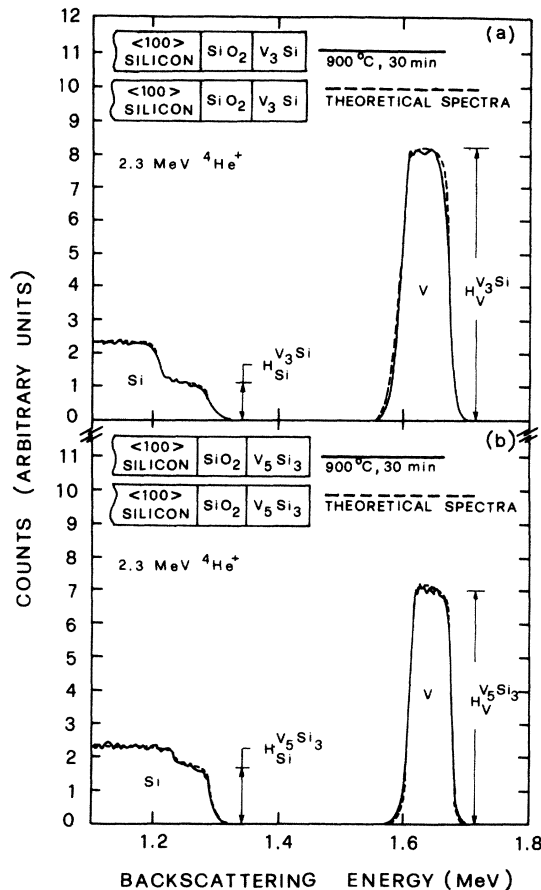


FIG. 1. Rutherford backscattering spectra of the as-deposited specimens pre-heat treated at 900°C for 30 min for (a) V₃Si, and (b) V₅Si₃, respectively. The dashed lines represent the superimposed theoretical spectra, while the horizontal bars indicate the corresponding silicon and vanadium profile heights.

III. RESULTS

A. Structural and compositional analysis

Figures 1(a) and 1(b) show the 2.3-MeV $^4\text{He}^+$ ions Rutherford backscattering spectra before and after heat treatment at 900°C for 30 min for V₃Si and V₅Si₃ specimens, respectively. The shapes do not change after heat treatment; this indicates that the as-deposited thin films are both uniform in depth, and of the correct stoichiometric ratio. The inner SiO₂/silicide interfaces remain sharp after heat treatment in all the cases examined, indicating that no reaction has occurred between the substrate and the silicide thin films.

Figures 2(a) and 2(b) show the RBS spectra of 2.3-MeV $^4\text{He}^+$ ions before and after heat treatment at 900°C for 30 min for the alloy and the bilayer specimens of VSi₂, respectively. From the heights of vanadium and silicon signals in Fig. 2(a) a stoichiometric ratio of 1:3 has been calculated for the as-deposited thin film. A heat treatment at 900°C for 30 min of the alloy promoted a partial segregation of the excess silicon, nonuniform in depth and

primarily towards the inner interface. In the case of bilayer specimens, all the V reacted with the Si during the heat treatment to form a VSi_2 thin film with a correct stoichiometric ratio of 1:2.

Figure 3 shows the XRD spectra of the V_3Si , V_5Si_3 , and VSi_2 compounds formed after heat treatment at 900°C for 30 min. The sharper peaks observed in the V_3Si and VSi_2 XRD spectra indicate an average grain size greater than that of V_5Si_3 (~ 300 Å), in agreement with TEM analysis.

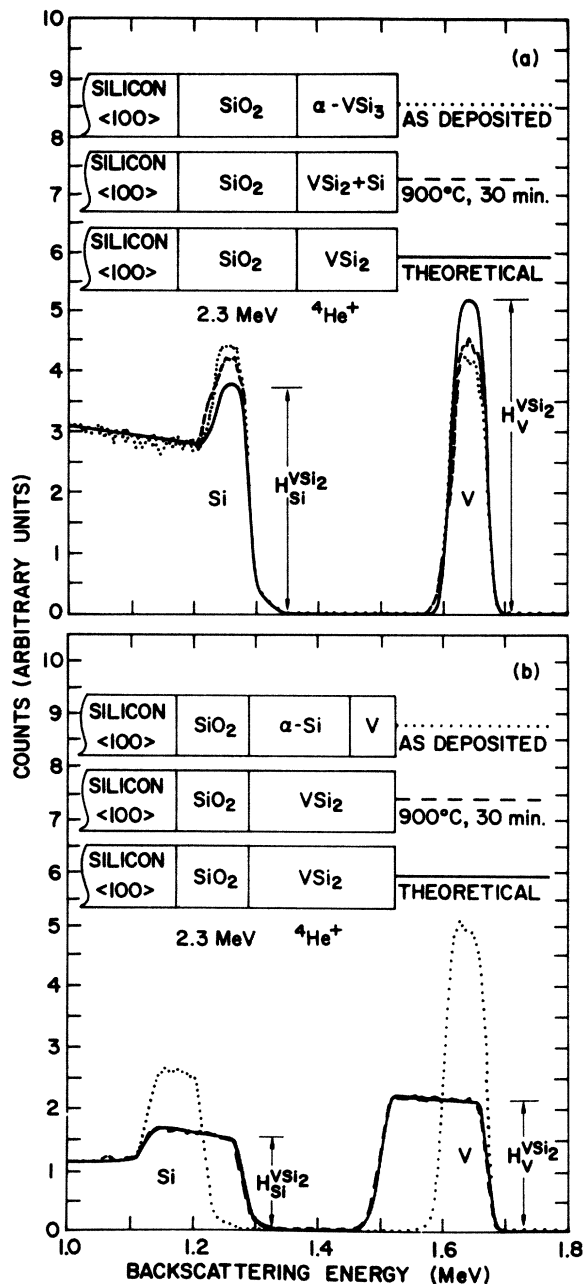


FIG. 2. Rutherford backscattering spectra of as-deposited specimens after heat treatment at 900°C for 30 min for (a) the alloy, and (b) the bilayer thin films of VSi_2 , respectively. The continuous lines represent the superimposed theoretical spectra of VSi_2 .

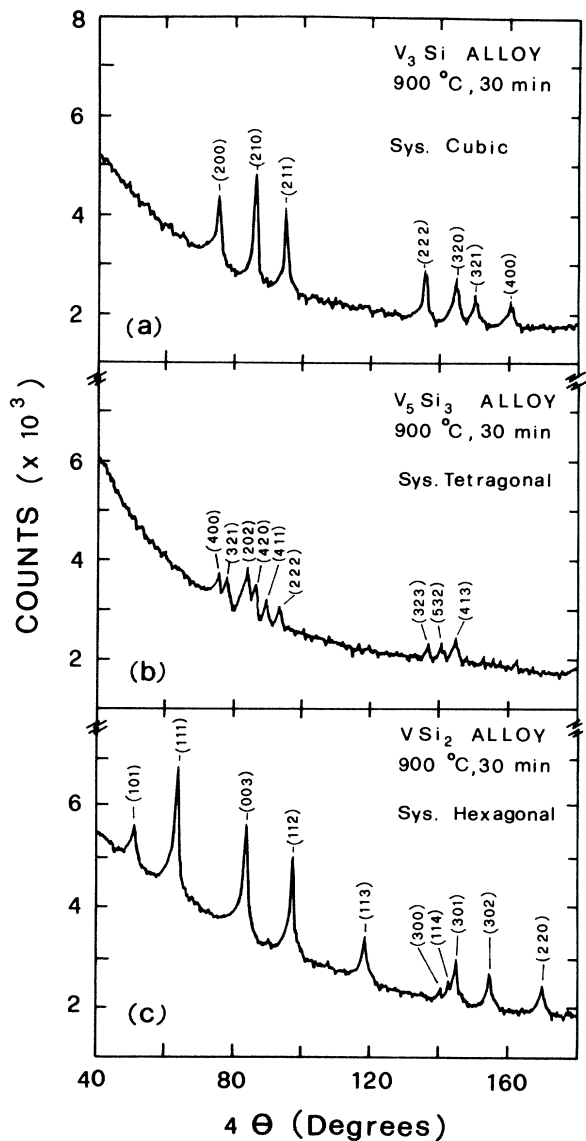


FIG. 3. Seeman-Bohlin x-ray diffraction spectra of (a) V_3Si alloy, (b) V_5Si_3 alloy, and (c) VSi_2 alloys specimens after isothermal heat treatment at 900°C for 30 min.

B. Resistivity measurements

For the heat-treated specimens, the measured temperature dependence of resistivity with a resolution of $\sim 10^{-4}$ in the temperature range of 2–1000 K is illustrated in Fig. 4. At high temperatures, $T \geq 200$ K, the resistivity behavior for the three compounds shows marked departure from the usual temperature dependence of both transition and nontransition metals,²² which is well described by the following:

$$\rho_{\text{ideal}}(T) = \rho_0 + \rho_1(T), \quad (1)$$

where ρ_0 is the temperature-independent residual resistivity due to the scattering processes with defects and impurities, and $\rho_1(T)$ is the phonon-scattering contribution, linear in the high-temperature limit. In Fig. 4 the ρ -

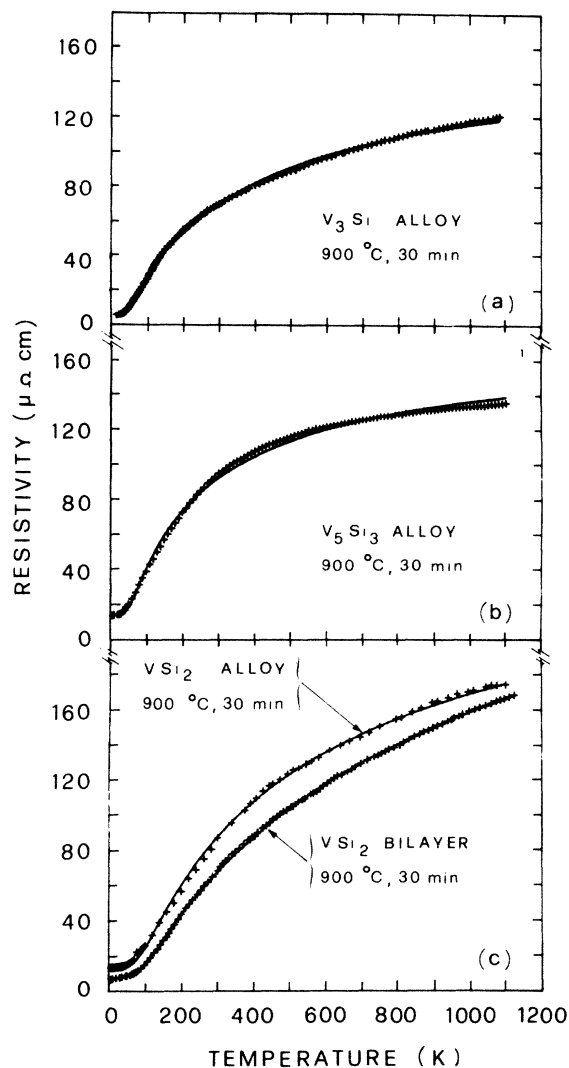


FIG. 4. Comparison between the experimental resistivity data (crosses) and the parallel resistor-model formula (solid line) with the parameters listed in Table I for the specimens heat treated at 900°C for 30 min of (a) V_3Si alloy, (b) V_5Si_3 alloy, and (c) VSi_2 alloy and bilayer, respectively.

versus- T curves show a negative deviation from linearity and a quasisaturation phenomenon at high temperatures. This behavior, similar to that previously reported for Nb (Ref. 13) as well as for several $A15$ compounds,^{23,24,14} Chevrel phases,^{14,15} and ternary borides,¹⁶ has been explained on the basis of the conduction-electron mean free

path approaching a lower limit with the consequent breakdown of the classical Boltzmann theory.²⁵ To describe this effect the phenomenologically shunt-resistor model has been proposed:¹³

$$1/\rho(T) = 1/\rho_{ideal}(T) + 1/\rho_{sat} \quad (2)$$

The use of the above parallel-resistor formula implies that

$$\lim_{T \rightarrow 0} \rho(T) = \rho_0 \left[\frac{\rho_{sat}}{\rho_0 + \rho_{sat}} \right],$$

i.e., the measured low-temperature limit is different from the ideal-temperature independent term ρ_0 . Due to the fact that this difference is very small, varying from 4% in V_3Si to 8% in V_5Si_3 , we will not distinguish between the ideal ρ_0 and the measured low-temperature limit of $\rho(T)$ in our analysis.

Allen and co-workers^{26,27} developed a "modernized Bloch-Grüneisen theory" for $\rho_{ideal}(T)$, closely related to the modern theory of superconductivity. This theory, which follows the basic variation solution of the Bloch-Boltzmann equation, leads to the classical Bloch-Grüneisen formula with a model employing Debye phonons, spherical Fermi surface and electron-phonon coupling via longitudinal phonons only, and no umklapp scattering.²⁸ The experimental data of Fig. 4 have been interpreted by approximating $\rho_{ideal}(T)$ in Eq. (2) with the Bloch-Grüneisen expression:

$$\rho_1(T) = \rho' TG(\Theta_R/T), \quad (3)$$

$$G(\Theta_R/T) = 4 \left[\frac{T}{\Theta_R} \right]^4 \int_0^{\Theta_R/T} dz \frac{z^5}{(e^z - 1)(1 - e^{-z})},$$

where Θ_R is the Debye temperature and ρ' the high-temperature limit of ρ_1/T . The best fit was achieved by minimizing the root-mean-square (rms) deviation, allowing the four parameters ρ_0 , ρ' , Θ_R , and ρ_{sat} to float. In Table I the set of parameters which minimize the rms error is reported for each of the three compounds. The solid curves in Fig. 4 are the calculated curves based on the shunt-resistor formula. The agreement with the experimental resistivity data is quite good.

Concerning the best-fit parameters, a few points must be emphasized. The higher value (almost 80%) measured for ρ_0 in the VSi_2 alloy than the VSi_2 bilayer is consistent with structural analysis (RBS, XRD, and TED), which shows that the former has a higher content of impurity (Si) and defects. They contribute mainly at low tempera-

TABLE I. Parameters used in Eqs. (1), (2), and (3) to fit the electrical resistivity curves of V_3Si , V_5Si_3 , and VSi_2 shown in Fig. 4.

Compounds	ρ_0 ($\mu\Omega$ cm)	ρ' ($\mu\Omega$ cm/K)	Θ_R (K)	ρ_{sat} ($\mu\Omega$ cm)	rms error ($\mu\Omega$ cm)
VSi_2 alloy	14.84	0.474	550.01	289.75	0.0201
VSi_2 bilayer	7.92	0.320	555.80	301.36	0.0166
V_5Si_3 alloy	15.36	0.677	345.09	169.76	0.0185
V_3Si alloy	6.19	0.424	299.71	158.17	0.0108

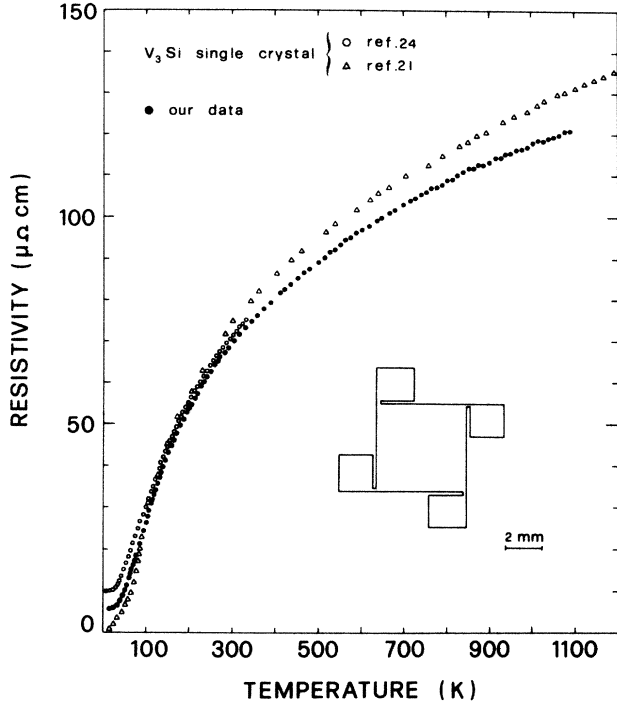


FIG. 5. Comparison between the resistivity data for V_3Si compounds obtained by Marchenko (Ref. 21) (open triangles), by Caton and Viswanathan (Ref. 24) (open circles), and those of the present work (solid circles). The inset shows the four-terminal van der Pauw pattern used for the electrical transport measurements of V_3Si alloy thin films.

tures to increase the scattering processes and consequently ρ_0 . The smallest average grain size determined by TEM in V_5Si_3 specimens can explain, in terms of grain-boundary scattering, the highest ρ_0 value measured for this compound.

Also, the Debye-temperature values are reasonable if compared to those reported for other silicides²⁻⁵ and to that calculated (300 K) by Caton and Viswanathan²⁴ by applying the same model to the resistivity data of V_3Si single crystals. Furthermore, the increasing values of Θ_R with the content of Si in the compounds are consistent with the predictions from the melting points²⁹ according to the Lindemann formula.²² It is worthwhile pointing out that the Debye temperature deduced for V_3Si from specific heat³⁰ is about 8% higher than that obtained by fitting $\rho(T)$; similar discrepancies have already been observed in several metals.³¹

Finally, the values of ρ_{sat} for the V-rich compounds are very similar to those ($\sim 150 \mu\Omega \text{ cm}$) reported for the A15-structure compounds,^{13,24} while the saturation resistivity found for VSi_2 ($\rho_{sat} \sim 300 \mu\Omega \text{ cm}$) is almost double. In the case of V_3Si , a comparison of our data to those of Marchenko²¹ and Canto and Viswanathan²⁴ is shown in Fig. 5, and the agreement in their saturation behavior is seen. Furthermore, the best-fit parameters of Caton and Viswanathan are very similar to ours.

The polycrystalline V_3Si thin films is a superconductor.

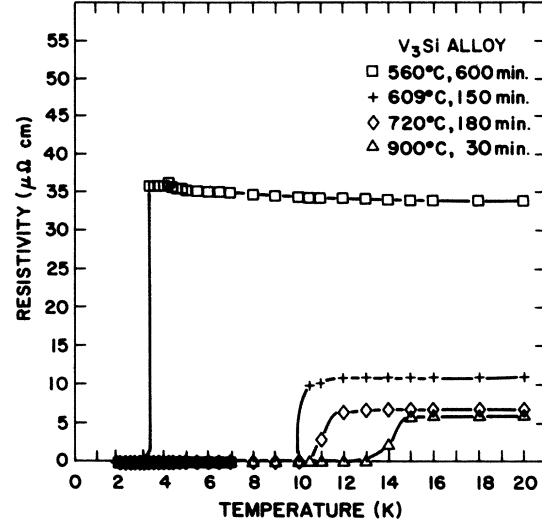


FIG. 6. Resistivity behavior versus temperature in the low-temperature regime for V_3Si alloy specimens heat treated at different temperatures and times. It is evident that there is the effect of the heat treatment on the transition temperature and the residual resistivity ratio. The solid lines have been added to connect the data points.

The low-temperature resistivity behavior of several samples heat treated at different temperatures are shown in Fig. 6. The transition from a normal to a superconducting state for the sample heat treated at 900°C for 30 min is characterized by a T_c about 15 K and by a width $\Delta T_c = 2$ K. The ΔT_c is defined as the width of a transition between 10% and 90% of the normal-state resistivity. The residual resistivity was $6.35 \mu\Omega \text{ cm}$ and the residual resistance ratio (RRR) was 10.6. This indicates that our V_3Si specimens are not free of defects. For the sample heat treated at 560°C , we noticed a slight increase in resistivity before the onset of superconductivity; most likely it is due to the scattering off V_3Si grains. Polycrystalline V_5Si_3 and VSi_2 thin films do not show any superconducting behavior down to 2 K.

C. Hall-coefficient measurements

The measured temperature dependence of the Hall coefficient (R_H) in the temperature range 10–350 K is shown in Fig. 7 for V_3Si , V_5Si_3 , and VSi_2 alloy thin films after a heat treatment at 900°C for 30 min. The temperature dependence of R_H for the VSi_2 bilayer specimen is not reported in Fig. 7 because it is nearly the same as the VSi_2 alloy specimen. The R_H value is positive and almost constant with temperature for V_3Si ; for V_5Si_3 it is always negative and strongly dependent on temperature, and for VSi_2 it is mainly negative and it changes sign at lower temperature. The observed change of R_H with temperature suggests the presence of a mixed conduction mechanism, holes being the predominant charge carriers in V_3Si , and the electrons in V_5Si_3 and VSi_2 . Similar temperature dependence of R_H has also been observed in $MoSi_2$,² $TaSi_2$,³² WSi_2 ,³² and $NbSi_2$.³³

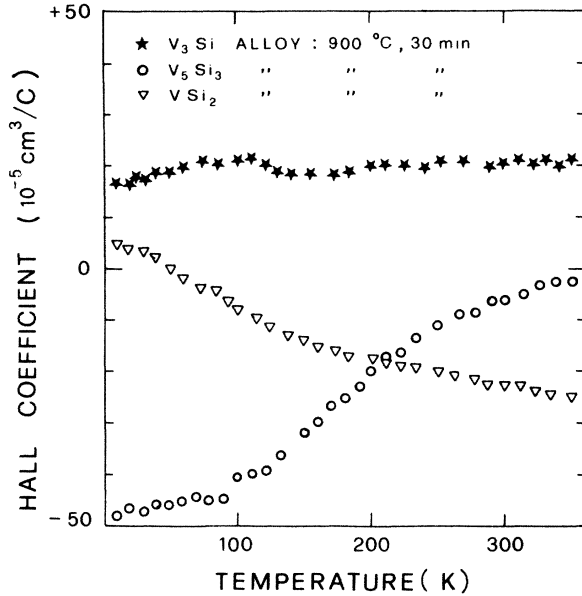


FIG. 7. Hall coefficient of V_3Si , V_3Si_3 , and VSi_2 alloy thin films heat treated at $900^\circ C$ for 30 min plotted as a function of temperature.

IV. DISCUSSION

The parameters which fit the experimental resistivity curves can be used to gain information about physical properties of the three compounds. According to Allen,³⁴ the electron-phonon resistivity parameter ρ' can be written as

$$\rho' = \frac{6\pi k_B \lambda_{tr}}{\hbar e^2 2N(0) \langle V_F^2 \rangle}, \quad (4)$$

where $2N(0)$ is the density of states at the Fermi level, $\langle V_F^2 \rangle$ is the mean-square electron velocity at the Fermi surface, k_B and \hbar are the Boltzmann and Planck constants, respectively, and λ_{tr} is the dimensionless electron-phonon coupling constant, which is closely related to the coupling constant λ that determines the superconducting transition temperature. In the case of Nb and Pd it has been found that λ_{tr} differs from λ by about 10%.²⁸

The value of ρ' depends on the three quantities: λ_{tr} , $N(0)$, and V_F . If an independent evaluation of any two of them is available, it is possible to calculate the third by knowing ρ' , and to obtain some other microscopic parameters of the materials. One of them is the electron mean free path $l_{e-ph}(T)$ whose value is temperature dependent due to the electron-phonon scattering processes and it is given by

$$l_{e-ph}(T) = \frac{\hbar V_F}{2\pi \lambda_{tr} k_B T G(\Theta_R/T)}. \quad (5)$$

The effective mass m^* , and the charge carrier density n can be evaluated respectively as

$$m^* = \left[\frac{\pi^2 \hbar^2 2N(0)}{V_F} \right]^{1/2}, \quad (6)$$

and

$$n = \frac{(m^* V_F)^3}{3\pi^2 \hbar^3}.$$

The breakdown of the classical Boltzmann theory in the case of resistivity saturation has been interpreted in terms of the Ioffe-Regel criterion:³⁵ The electron mean free path $l_{e-ph}(T)$ cannot be shorter than the interatomic distance a . It implies the existence of a minimum time between collisions, $\tau_0 = a/V_F$, so that no collisions happen for $\tau < \tau_0$.²³ By using the computed V_F from Eq. (4) with known ρ' , λ_{tr} , and $N(0)$ and the nearest-neighbors distance in the compounds, we found $\tau_0(V_3Si) = 57.14$ a.u. and $\tau_0(VSi_2) = 35.68$ a.u.

A theoretical estimate of ρ_{sat} may be obtained from the free-electron model using τ_0 :

$$\rho_{sat} = (\sigma_{sat})^{-1} = \left[\frac{e^2 n \tau_0}{m^*} \right]^{-1}. \quad (7)$$

We found 335 and 614 $\mu\Omega$ cm for V_3Si and VSi_2 , respectively. By comparing these results with the fitting parameters of Table I, it shows that the free-electron formula of Eq. (7) overestimates¹⁷ ρ_{sat} by a factor of two, but it correctly predicts the increase on going from V_3Si to VSi_2 , which is mainly due to the difference in the electron concentration.³⁶

From the knowledge of the residual resistivity ρ_0 it is possible to compute the elastic scattering length l_e due to carrier scattering by structural defects and impurities:

$$l_e = \frac{m^* V_F}{ne^2 \rho_0}. \quad (8)$$

For V_3Si and VSi_2 we have made an independent estimate of $2N(0)$ and λ_{tr} in order to evaluate V_F . For V_3Si , a value of 1.12 for λ has been obtained from the literature³⁷ by assuming $\lambda_{tr} = \lambda$. For VSi_2 , we determine $\lambda = 0.7$ by taking $2N(0) = 0.54$ electrons/(eV atom) and $E_F = 13.6$ eV.^{21,38}

In Table II the calculate value of V_F , $l_{e-ph}(300\text{ K})$, m^* , n , and l_e for the annealed V_3Si alloy and VSi_2 alloy and bilayer specimens are reported. Our estimates of the mean electron velocity at the Fermi surface are very reasonable. They may be compared with the value of $2.1\text{--}2.2 \times 10^7$ cm/sec found in A15 compounds.³⁹ Also a first-principles calculation of V_F for V_3Si (Ref. 40) gives a value of 1.72×10^7 cm/sec, in excellent agreement with our estimate.

We emphasize that the values calculated for $l_{e-ph}(T)$ are consistent with the idea of a saturation in resistivity and can describe the different resistivity behavior observed in the two compounds. In the case of V_3Si , $l_{e-ph}(300\text{ K})$ of 6.6 Å is comparable to the corresponding value of 5–6 Å found in other A15 compounds³⁹ and comparable to the order of magnitude of the interatomic distance. These results confirm the fact that in these compounds, the Bloch's theory, based on extended states, is not applicable

TABLE II. The transport parameters l_{e-ph} , V_F , m^* , n , and l_e estimated for V_3Si and VSi_2 compounds by using the best-fit parameters of Table I.

Compound	V_F (cm/sec)	$l_{e-ph}(300\text{ K})$ (Å)	m^*	l_e (Å)	$n(\text{cm}^{-3})$
V_3Si alloy	1.7×10^7	6.6	8.4	128	6.5×10^{22}
VSi_2 alloy	2.5×10^7	15	3.9	126	2.0×10^{22}
VSi_2 bilayer	2.9×10^7	19	3.5	194	2.4×10^{22}

already at room temperature and the metal is expected to approach the saturation regime. The greater values of $l_{e-ph}(T)$ calculated at room temperature for both specimens of VSi_2 are also consistent with the experimental data, where the saturation is being observed at higher temperatures. Only at 900 K, the phonon-limited mean free path, of the order of 5 Å, is comparable to the interatomic distance.

The high value of m^* found in V_3Si and VSi_2 is consistent with the presence of d states near E_F in these materials, while the characteristic flatness of the bands in $A15$ V_3Si (Ref. 41) is responsible for the higher value found in this compound than in VSi_2 .

The charge-carrier density values²¹ shown in Table II correspond to about three carriers and one carrier per molecule for V_3Si and VSi_2 , respectively. They are consistent with the Hall data n_H which, with allowances made for the probable existence of carriers of both signs, give a room-temperature carrier density of $3 \times 10^{22} \text{ cm}^{-3}$ and $2.97 \times 10^{22} \text{ cm}^{-3}$ for VSi_2 and V_3Si , respectively. Furthermore, these values of n are of comparable magnitude to those calculated by Hensel *et al.*³ for $CoSi_2$ and $NiSi_2$.

Concerning the elastic scattering length, its decrease by 50% from VSi_2 bilayer to VSi_2 alloy is due to the silicon impurities which are present in the alloy specimens even after heat treatments at high temperatures.

Although the saturation resistivity model has given consistent values of mean free paths and other physical parameters of the compounds, the model may not necessarily be unique in describing their conduction behavior. It has been pointed out that such a model has failed to explain the negative temperature coefficient of resistivity observed in many disordered materials of very short mean free paths.⁴² However, Mooij expressed the idea that a partial electron localization may be the cause of the negative $d\rho/dT$ observed.⁴³ This behavior can be formally included in the parallel-resistor model by allowing for the number of nonlocalized electrons to decrease at low temperatures.¹⁴ We note that a discussion of a localization

model which can handle both positive and negative $d\rho/dT$ in many disordered metals has been given in Ref. 44. Clearly the saturation phenomenon is still a subject worth studying and the data presented here will be valuable in examining other models.

V. CONCLUSIONS

We have measured the temperature dependence of the resistivity and of the Hall coefficient of V_3Si , V_5Si_3 , and VSi_2 thin films. The wide temperature range (2–1100 K) used in the study of ρ versus T allowed us to observe an anomalous metallic behavior common to the three compounds. The intrinsic resistivity exhibits a strong negative curvature and approaches a saturation value at high temperatures. This phenomenon has been interpreted in the framework of the parallel-resistor model which includes the electron-phonon scattering model of Bloch-Grüneisen to account for the ideal contribution to the total resistivity. The best fits to the resistivity curves over the entire temperature range are quite good and the parameters used to achieve the fitting are physically reasonable. Furthermore, the electron mean free paths calculated at room temperature for V_3Si (6.6 Å) and VSi_2 (~19 Å) are consistent with the experimental data and the theoretical model. The behavior of Hall coefficients is complicated, suggesting the presence of both electrons and holes with different temperature dependences of their mobilities.

ACKNOWLEDGMENTS

The authors gratefully acknowledge the Central Scientific Service Materials Laboratory staff at Yorktown for specimen preparation, P. A. Saunders for Rutherford backscattering spectrometry, H. Takai (Tokyo Denki University) for TED and TEM analysis, J. A. Lacey for low-temperature electrical measurements, P. A. Psaras for technical assistance, and C. C. Tsuei for helpful discussions.

*Permanent address: Department of Physics, University of Modena, Via Campi 213/A 41100 Modena, Italy.

¹K. N. Tu and J. W. Mayer, in *Thin Films—Interdiffusion and Reactions*, edited by J. M. Poate, K. N. Tu, and J. W. Mayer (Wiley-Interscience, New York, 1978), p. 359.

²P. H. Woerlee, P. M. Th.M. van Attekum, A. A. M. Hoeben,

G. A. M. Hurk, and P. A. M. Wolters, *Appl. Phys. Lett.* **44**, 876 (1984).

³J. C. Hensel, R. T. Tung, J. M. Poate, and F. E. Unterwald, *Appl. Phys. Lett.* **44**, 913 (1984).

⁴J. C. Hensel, R. T. Tung, J. M. Poate, and F. C. Unterwald, *Phys. Rev. Lett.* **54**, 1840 (1985).

- ⁵V. Malhotra, T. L. Martin, M. T. Huang, and J. E. Mahan, *J. Vac. Sci. Technol. A* **2**, 271 (1984).
- ⁶Z. Fisk and A. C. Lawson, *Solid State Commun.* **13**, 277 (1973).
- ⁷M. P. Sarachik, G. E. Smith, and J. H. Wernick, *Can. J. Phys.* **41**, 1542 (1963).
- ⁸G. Webb, Z. Fisk, J. E. Englehardt, and S. D. Bader, *Phys. Rev. B* **15**, 2624 (1977).
- ⁹M. Gurvitch, H. K. Ghosh, B. L. Gyorffy, H. Lutz, O. F. Kammerer, J. S. Rosner, and Myron Strongin, *Phys. Rev. Lett.* **41**, 1616 (1978).
- ¹⁰P. J. Cote and L. V. Meisel, *Phys. Rev. Lett.* **40**, 1586 (1978).
- ¹¹B. Chakraborty and P. B. Allen, *Phys. Rev. Lett.* **38**, 782 (1979).
- ¹²Z. Fisk and G. W. Webb, *Phys. Rev. Lett.* **36**, 1084 (1976).
- ¹³H. Wiesmann, M. Gurvitch, H. Lutz, A. Ghosh, B. Schwartz, M. Strongin, P. B. Allen, and J. W. Halley, *Phys. Rev. Lett.* **38**, 782 (1977).
- ¹⁴C. S. Sunandana, *J. Phys. C* **12**, L165 (1979).
- ¹⁵R. Martin, K. R. Mountfield, and L. R. Corruccini, *J. Phys. (Paris) Colloq.* **39**, C6-371 (1978).
- ¹⁶J. M. Rowell, R. C. Dynes, and P. H. Schmidt, in *Superconductivity in d- and f-Band Metals*, edited by H. Suhl and M. B. Maple (Academic, New York, 1980), p. 409.
- ¹⁷B. P. Schweiss, B. Renker, E. Schneider, and W. Reichardt, in *Superconductivity in d- and f-Band Metals—Second Rochester Conference*, edited by D. H. Douglass (Plenum, New York, 1976).
- ¹⁸B. M. Klein and L. L. Boyer, in *Superconductivity in d- and f-Band Metals*, edited by H. Suhl and M. B. Maple (Academic, New York, 1980).
- ¹⁹O. Bisi and L. W. Chiao, *Phys. Rev. B* **25**, 4943 (1981).
- ²⁰G. Oya, H. Inabe, Y. Onodera, Y. Sawada, and Y. Onodera, *J. Appl. Phys.* **53**, 115 (1984); G. Oya, K. Akada, J. Kazumi, Y. Sawada, and Y. Onodera, *ibid.* **56**, 177 (1984).
- ²¹V. A. Marchenko, *Fiz. Tverd. Tela (Leningrad)* **15**, 1893 (1973) [*Sov. Phys.—Solid State* **15**, 1261 (1973)].
- ²²J. M. Ziman, *Electrons and Phonons* (Oxford University Press, London, 1960).
- ²³M. Gurvitch, *Phys. Rev. B* **24**, 7404 (1981).
- ²⁴R. Caton and R. Viswanathan, *Phys. Rev. B* **25**, 179 (1982).
- ²⁵P. B. Allen and B. Chakraborty, *Phys. Rev. B* **23**, 4815 (1981).
- ²⁶P. B. Allen, *Phys. Rev. B* **3**, 305 (1971).
- ²⁷P. B. Allen and W. H. Butler, *Phys. Today* **31**(12), 44 (1978).
- ²⁸F. J. Pinski, P. B. Allen, and W. H. Butler, *Phys. Rev. B* **23**, 5080 (1981).
- ²⁹S. P. Murarka, *Silicides for VLSI Applications* (Academic, New York, 1983).
- ³⁰R. Viswanathan and R. Caton, *Phys. Rev.* **18**, 15 (1978).
- ³¹F. J. Blatt, *Physics of Electronic Conduction in Solids* (McGraw-Hill, New York, 1968).
- ³²F. Nava (unpublished).
- ³³F. Nava, P. A. Psaras, H. Takai, K. N. Tu, S. Valeri, and O. Bisi, *J. Mater. Res.* **1**, 327 (1986).
- ³⁴P. B. Allen, *Phys. Rev. B* **17**, 3725 (1978).
- ³⁵A. F. Ioffe and A. R. Regel, *Prog. Semicond.* **4**, 237 (1960).
- ³⁶We note that Gurvitch (Ref. 23) obtained a value of $122 \mu\Omega \text{ cm}$ for ρ_{sat} of V_3Si . This lower value is mainly due to the use of the cube length instead of the first-neighbor distance used in this paper for the interatomic distance. This result gives an indication of amount of uncertainty of these estimations for ρ_{sat} .
- ³⁷S. V. Vonsovsky, Yu. A. Izyumov, and E.-Z. Kurmaev, *Superconductivity of Transition Metals* (Springer-Verlag, Berlin, 1982).
- ³⁸I. R. Gomersall and B. L. Gyorffy, *Phys. Rev. Lett.* **33**, 1286 (1974).
- ³⁹P. B. Allen, W. E. Pickett, K. M. Ho, and M. L. Cohen, *Phys. Rev. Lett.* **40**, 1532 (1978).
- ⁴⁰B. M. Klein, *Superconductivity in d- and f-band Metals*, edited by H. Suhl and M. Brian (Academic, New York, 1980).
- ⁴¹L. F. Mattheis, *Phys. Rev. B* **12**, 2161 (1975).
- ⁴²P. A. Lee and T. V. Ramakrishnan, *Rev. Mod. Phys.* **57**, 287 (1985).
- ⁴³H. Mooij, *Phys. Status Solidi A* **17**, 521 (1973).
- ⁴⁴C. C. Tsuei, *Bull. Am. Phys. Soc.* **31**, 594 (1986).